Simulation pathway for estimating heat island influence on urban/suburban building space-conditioning loads and response to facade material changes

Kanchane Gunawardena [a,*], Tristan Kershaw [b], Koen Steemers [a]

[a] *The Martin Centre of Architectural and Urban Studies, Department* of *Architecture, University of Cambridge, 1-5 Scroope Terrace, Cambridge, CB2 1PX, United Kingdom.*
[b] *Department of Architecture and Civil Engineering, University of Bath, Claverton Down, Bath, BA2 7AY, United Kingdom.*

**Corresponding author: krag2@cam.ac.uk*

ABSTRACT

Environmental thermal loading on urban buildings is expected to increase owing to the combined influence of a warming climate, increasing frequency and severity of extreme heat events, and the urban heat island (UHI) effect. This paper presents how a computationally efficient estimation pathway could be utilised to understand UHI influence on building energy simulations. As an example, this is examined by considering UHI influence on the space-conditioning loads of office buildings within urban and suburban conditions, and how the trend of replacing heavyweight facades with lightweight alternatives could affect their surrounding microclimates, as well as building energy use. The paper addresses this through simulations of street canyons based on the urban Moorgate and suburban Wimbledon areas of London. Results show that with all scenarios including the UHI within a dynamic thermal simulation presents between 2.5 to 9.6 % net increase in annual space-conditioning. The study also demonstrates that the trend in urban centres to replace heavyweight facades with lightweight insulated alternatives increases space-conditioning loads, which in turn increases UHI intensity to create a warming feedback loop. The study therefore stresses the significance of including microclimate loading from the UHI in estimating urban and suburban energy use, and the combined simulation approach is presented as a computationally efficient pathway for use by built environment designers.

Keywords: Heat island effect; space-conditioning loads; facade materials; urban energy use; suburban energy use

1. Introduction

Climate change influences such as the increasing frequency and severity of extreme heat events present critical challenges to the continuing global urbanisation trend [1]. This is complicated further by the long-established effects of the urban heat island (UHI) [2,3]. Such enhanced climatic loads can exert significant influence on the sustainable operation of urban settlements. Understanding the interactions between the built-environment and its dynamic climate is therefore necessary for delivering sustainable cities.

Urban climate interactions have long been identified as being governed by the 'urban energy balance' that represents the partitioning of energetic exchanges of the urban surface system [4]. The warmer climate often experienced in cities is explained by a net positive thermal balance that arises from changes made to its surface properties; including increased surface roughness [3], use of high heat storage and low albedo materials [5], reduced green and blue-space for evapotranspiration [5,6], and increased heat and pollution generated from human activities [3]. The UHI effect that results is an additional environmental thermal load that affects how energy is used within buildings [7], which in turn feedbacks to the UHI as anthropogenic emissions [5,8]. Higher building energy use for space-conditioning for example could contribute to the greater storage of thermal energy within urban systems, thereby helping to generate and intensify UHIs [3], and create a warming feedback-loop that leads to ever-worsening and unhealthy urban environments [9,10].

It should be noted that the UHI is not always a negative influence on building energy loads. The UHI typically represents a shift in time as well as magnitude of minimum and maximum temperatures, this can for instance result in a reduction in heating loads or the offsetting of peak temperatures beyond normal active hours. As such the interaction between the UHI and building space-conditioning loads is inherently complex, and further complicated by modern

construction practices adopting a trend towards favouring insulated lightweight solutions relative to traditional heavyweight materials in the interest of achieving greater speed and off-site assembly benefit [11,12].

1.1. Preceding work on London's UHI

The earliest UHI observations recorded are of London, England (maritime climate), where Howard [2] published timeseries data spanning a decade of measurements to identify the city to be 0.6 K warmer in the summer month of July and 1.2 K warmer in the winter month of November than the surrounding countryside. Howard [2] also observed that at night the city was 2.05 K warmer, while during the day it was 0.18 K cooler to demonstrate a modest cool island effect (relatively less warmer than the surrounding context) [13]. The relative urban warming of London has since been furthered by several longitudinal studies to demonstrate significant trends. Examining data from the more suburban site of Kew Gardens relative to a rural site at Rothamsted between 1878 and 1968, Moffitt [14] identified a ~0.8 K mean temperature increase, while timeseries analysis of central London meteorological data between 1931 and 1960 by Chandler [15] identified the annual mean to be warmer by 1.4 K, with a monthly mean value of 1.6 K for summer and 1.2 K for winter [13]. Recent timeseries analysis of central London between 1962 and 1989 by Lee [16] had identified the warming trend to have increased in relation to minimum temperatures, while maxima had decreased, and mean temperatures had remained constant. Furthermore, Lee [16] found that the daytime mean summertime heat island to have decreased from ~0.5 to 0.25 K, and the night-time heat islands to have increased by ~0.5 K. Wilby [17] broadly found similar results considering the period between 1958 and 1998, while the Jones & Lister [18] study considering data from several central sites also found that the relative increasing warming trend noted for periods earlier in the twentieth century to have stabilised in recent times. At Heathrow for example, they noted that mean temperatures had increased by 0.4 K between the start of the record in 1949 and 1980, although since 1981 the UHI had remained constant. Considering these observations, similar central London sites are projected as likely to maintain their UHI intensities in the future, while sites in suburban London are hypothesised to show an increase [18]. A significant factor affecting this trend is related to the radial distance from the core of the city [17,19]. Watkins *et al.* [13] found that 77 % of the variance of the mean night-time temperature measured across London to strongly correlate to the radial distance of each location, although daytime data presented a weaker association. They found the radial centre or thermal core to be in the City of London, characterised by its high-density development and high anthropogenic emissions [13]. These observations suggest that the transition between different morphologies and materiality typically observed when traversing from urban core to the peripheries as significant factors affecting the potency of the UHI load experienced at specific localities, with changes following densification trends to influence future UHI intensification.

London's UHI maxima and minima are addressed in detail by higher resolution studies typically of central sites that have been monitored for limited periods. For example, Watkins *et al.* [13] presented observational data from 1999 to show summertime peaks of ~7 K. Data from 1999 also demonstrated a maximum summer daytime UHI of 8.9 K, while a nocturnal maximum of 8.6 K was observed during clear-sky periods with low (<5 ms^{-1}) wind velocity [20]. Notably higher summertime nocturnal UHI peaks of 10 K were also reported on certain nights by a recent study of west London urban parks [21]. In winter, data gathered by Giridharan & Kolokotroni [22] showed that the maximum UHI to be 9 K for both day and night under low (<5 ms^{-1}) wind conditions. These examples highlight ample evidence for UHI maxima reaching significantly high values at central sites in the city. However, a comparison between London's urban core and the suburbs is difficult to consider given that such studies seldom attempt to discuss the intermediary condition represented by suburban localities.

1.2. Simulating an urban climate

Sourcing measurement data from direct techniques (using eddy flux stations with anemometers, thermocouples, gas analysers etc.) to compile localised weather profiles offer the most accurate means of accounting for site-specific climate loading. For such measurements to be representative, longitudinal data collection is necessary to account for the spatial and temporal diversity of UHI influence [3]. This requirement favours methodologies utilising relatively high-resolution networks of fixed stations as opposed to mobile traverse observations that offer only cross-sectional data. There is however no general scheme or accepted standard practice to direct such fixed-station measurement currently in place in cities [7]. This means that proposed studies would have to setup their own networks at the representative resolution required. Although such measurement projects exist [e.g. 13–15], the infrastructural cost to achieve similar programs of data collection are unlikely to be available for typical urban climate assessments [26]. As an alternative, data collected from private networks and enthusiasts (community-based data sharing) may be considered. This data however is likely to be inconsistent, with limited and divergent parameters collected, or include data gaps that would in turn require laborious interpolation methods to complete.

In order to approximate urban climate processes and influences, this study instead utilises a modified version (V5.1.0 *beta,* [27]) of the multiscale coupled framework published as the 'Urban Weather Generator' or UWG, V4.1.0 [28,29]. This framework is based on multiscale energy balances and Monin-Obukhov similarity theory, and is composed of four coupled sub-models that include a Rural Station Model (RSM), Vertical Diffusion Model (VDM), Urban Boundary Layer Model (UBLM), and an Urban Canopy and Building Energy Model (UC-BEM) based on the Masson [30] Town Energy Balance scheme and a building energy model developed by Bueno *et al.* [31]. A summary of the principal data exchanges is schematically presented in Fig. 1a, while detailed descriptions are offered in Bueno *et al.* [29,32], and field data verifications from Basel, Toulouse, and Singapore presented in Bueno *et al.* [29,32] and Nakano *et al.* [33]. The framework is primed with the input of a rural weather file, which is used by the sub-models to calculate canyon-specific temperature and humidity values to compile a modified canyon weather file in the EnergyPlus (*.epw*) format. This output weather file can then be used by dynamic building thermal modelling software to simulate indoor environmental conditions, space-conditioning loads, and building energy use. The updated version of the UWG (V5.1.0 *beta,* [27]) used in this study included restructuring to enhance input and computational efficiency, along with material definition improvements to provide flexibility to assess different material configurations. As these updates were concerned with improving input accuracy and range and not the simulation engine and its governing equations, the UWG's published error margin could be regarded as unaltered.

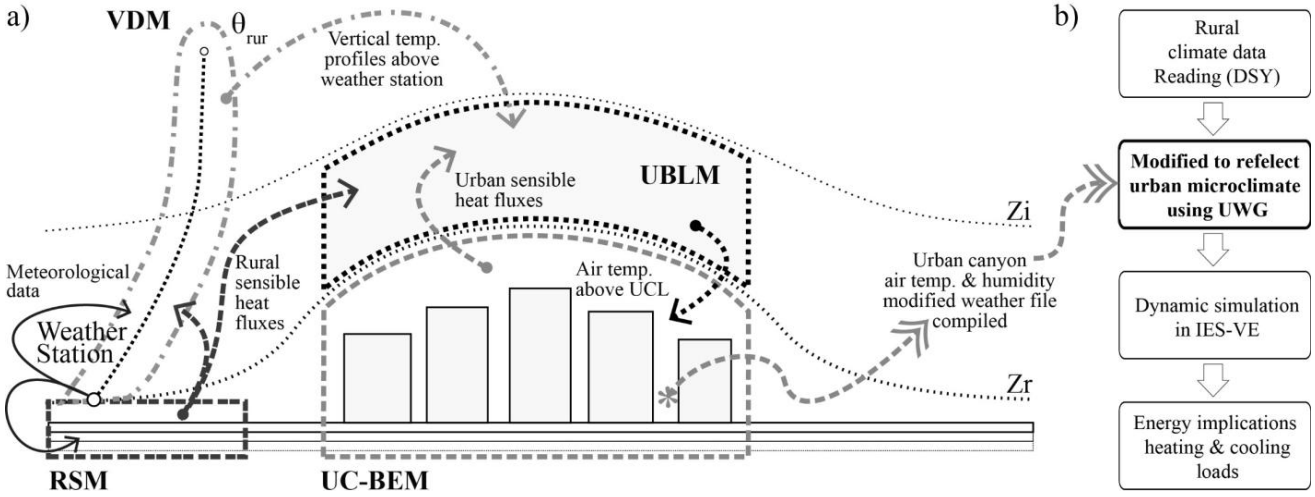

Fig. 1. Physical domain of UWG modules and data exchanges in an ideal city, based on Bueno *et al.* [29] (**a**); and method pathway for this study (**b**).

The purpose of this study is to present a computationally efficient pathway to estimate UHI influence on building energy simulations, with urban and suburban office building space-conditioning used as an exemplar assessment condition. A comparison between 'heavyweight' and 'lightweight' construction build-ups situated within the morphological contexts of Moorgate (central urban) and Wimbledon (suburban) areas of London are considered. To achieve this in a manner that is not reliant on site-specific measured data and suitable for wider applicability, the study presents the combined approach of using the above multiscale coupled urban climate framework (UWG) and a building energy model as a simplified and computationally efficient simulation pathway.

2. Methodology

The case study morphologies used for this study are of Moorgate and Wimbledon areas of London (see Fig. 2). Moorgate represents the central urban condition and is located in the City of London (the thermal core as identified by Watkins *et al.* [13]). It is regarded as a financial centre that includes many investment banks housed in traditional and contemporary office buildings. The traditional buildings notably present Portland stone facades, while some of the newer additions represent a dominance of glazing. Wimbledon in contrast represents the suburban condition located in southwest London and is generally represented by residential and retail buildings with dominant brick facades. Although there are expansive green-spaces in Wimbledon (i.e. the Common), the area selected for study represents a mainly residential neighbourhood of moderate density.

In this study, the above case study morphologies are idealised by averaging parameters to generate roughness profiles with a 500 m characteristic radius. At both sites, the canyon buildings are given the same occupancy profile of a medium-sized office building, and only differ between scenarios described in Table 1 in terms of their facade constructions as detailed in Appendix: Table A. 1. Note that care must be given to the accuracy of key sensitivity parameters identified in Appendix: Table A. 1, as errors with these values are likely to amplify deviations to result in false output. The roughness and material profiles scripted, together with a rural weather file are then input to the UWG (V5.1.0 *beta*) and run to generate new weather files that include the UHI influence on air temperature and humidity values for the canyon scenarios (see Fig. 1b). Priming simulations and output comparison with historical profiles is typically necessary to ensure characteristic UHI profiles are generated.

Fig. 2. Typical 'central urban' street canyon view of Moorgate (**a**); and 'suburban' street canyon view of Wimbledon, London (**b**); images from ©Google Earth, Street-view 2018.

The rural weather data used for this study is the Design Summer Year (DSY) for the Reading area created using the UKCP09 Weather Generator, the full methodology of which is described in Eames *et al.* [34]. The Reading area was selected for this purpose as it represents conditions beyond urbanised London (~60 km and ~52 km due west of the Moorgate and Wimbledon sites respectively), with previous research having demonstrated negligible contribution from the city of Reading's UHI to this gridded data output of the UKCP09 Weather Generator [35]. The generated weather data input therefore represents the rural boundary condition, where the influence of the city is assumed negligible. It also satisfied the criterion of presenting relatively clear (minimal cloud cover) conditions for both the summer and winter solstice, which represents ideal conditions for UHI formation and serve as benchmark days to compare and assess the different heat island scenarios generated.

The resulting UWG profiles were then applied to respective thermal models of the Moorgate and Wimbledon street canyons and their surrounding buildings, created using the dynamic simulation platform IES-VE [36] to estimate space-conditioning loads (see Fig. 1b).

Table 1.
Simulation scenarios considered.

	Weather file used	**Constructions used**
Urban (*Urb*)		
Urb-Base Stone	Unmodified Reading DSY.	*Default heavyweight scenario:* Using stone facades with glazing ratio (GR) of 0.30, detailed in Appendix: Table A. 1 (currently dominant among buildings of Moorgate).
Urb-Stone	Above modified using the UWG, i.e. with dominant construction of Stone facades and resulting UHI influence included.	
Urb-Base Glazed	Unmodified Reading DSY.	*Lightweight upgrade scenario:* Using glazed facades with GR of 0.30, detailed in Appendix: Table A. 2 (hypothetical).
Urb-Glazed	Above modified using the UWG, i.e. with dominant construction of Glazed facades and resulting UHI influence included.	

	Weather file used	Constructions used
Urb-Brick *Urb-Timber*	DSY for Reading modified using the UWG, i.e. with dominant construction of brick/timber facades and resulting UHI influence included.	*Material switch scenarios:* Using brick/timber facades with GR of 0.30, detailed in Appendix: Table A. 1 & Table A. 2 (hypothetical).
Suburban (*SUrb*)		
SUrb-Base brick *SUrb-Brick*	Unmodified Reading DSY. Above modified using the UWG, i.e. with dominant construction of brick facades and resulting UHI effect included.	*Default heavyweight scenario:* Using brick facades with GR of 0.30, detailed in Appendix: Table A. 1 (currently dominant among buildings of Wimbledon).
SUrb-Base Timber *SUrb-Timber*	Unmodified Reading DSY. Above modified using the UWG, i.e. with dominant construction of white-painted timber facades and resulting UHI effect included.	*Lightweight upgrade scenario:* White-painted timber facades with GR of 0.30, detailed in Appendix: Table A. 2 (hypothetical).
SUrb-Stone *SUrb-Glass*	DSY for Reading modified using the UWG, i.e. with dominant construction of stone/glass facades and resulting UHI influence included.	*Material switch scenarios:* Using stone/glass facades with GR of 0.30, detailed in Appendix: Table A. 1 & Table A. 2 (hypothetical).

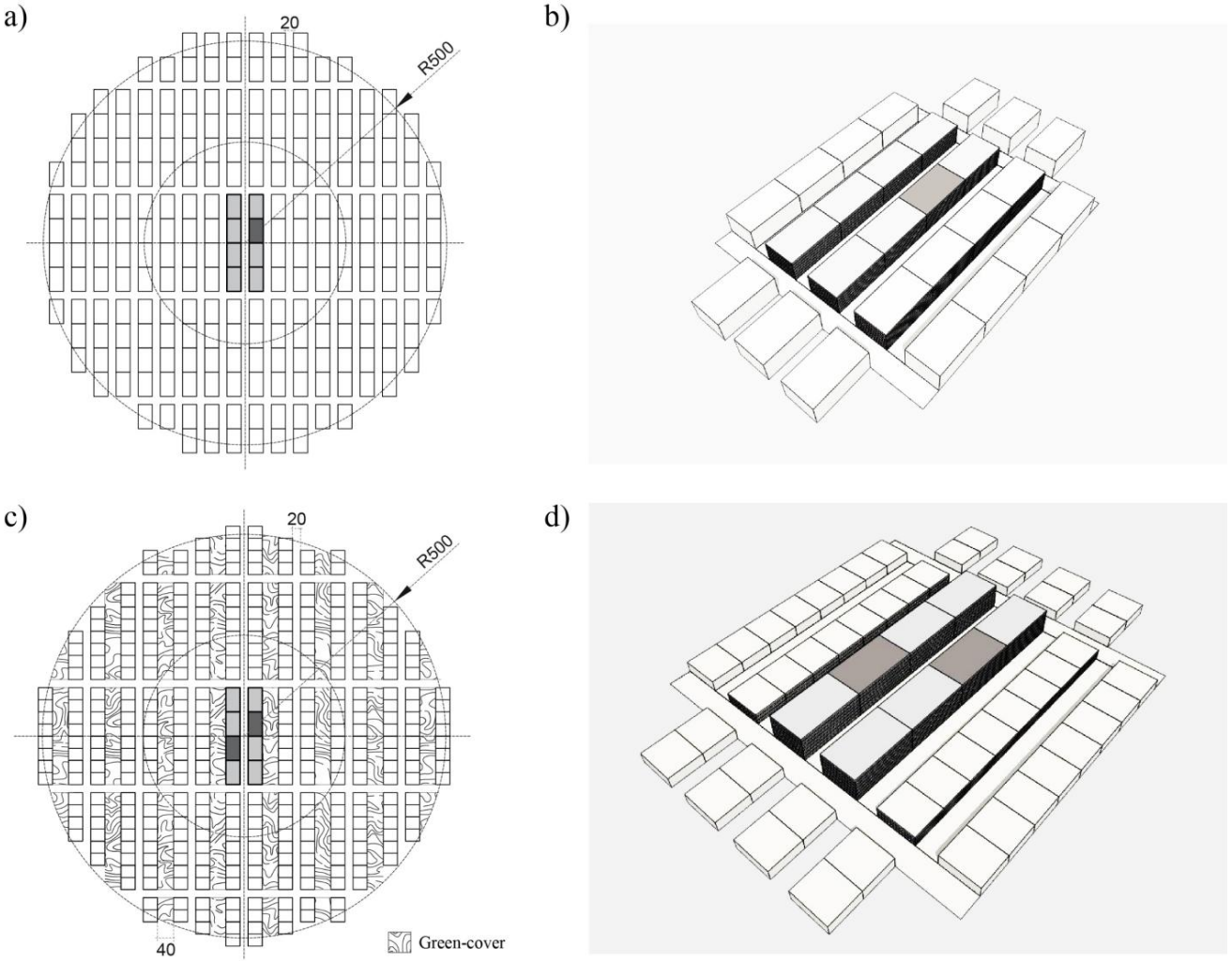

Fig. 3. Idealised radial area of the central urban condition based on Moorgate (**a**) and suburban condition based on Wimbledon (**c**) used for UWG microclimate generation (left), and corresponding focused street canyon models (**b** & **d**) used for IES-VE energy simulations (right).

3. Results

The following presents firstly, the features of the weather files generated by the UWG with the UHI influence included; secondly, their resulting external building surface temperatures; and finally, indoor space-conditioning loads for buildings that belong to the Moorgate and Wimbledon street canyons highlighted in Fig. 3.

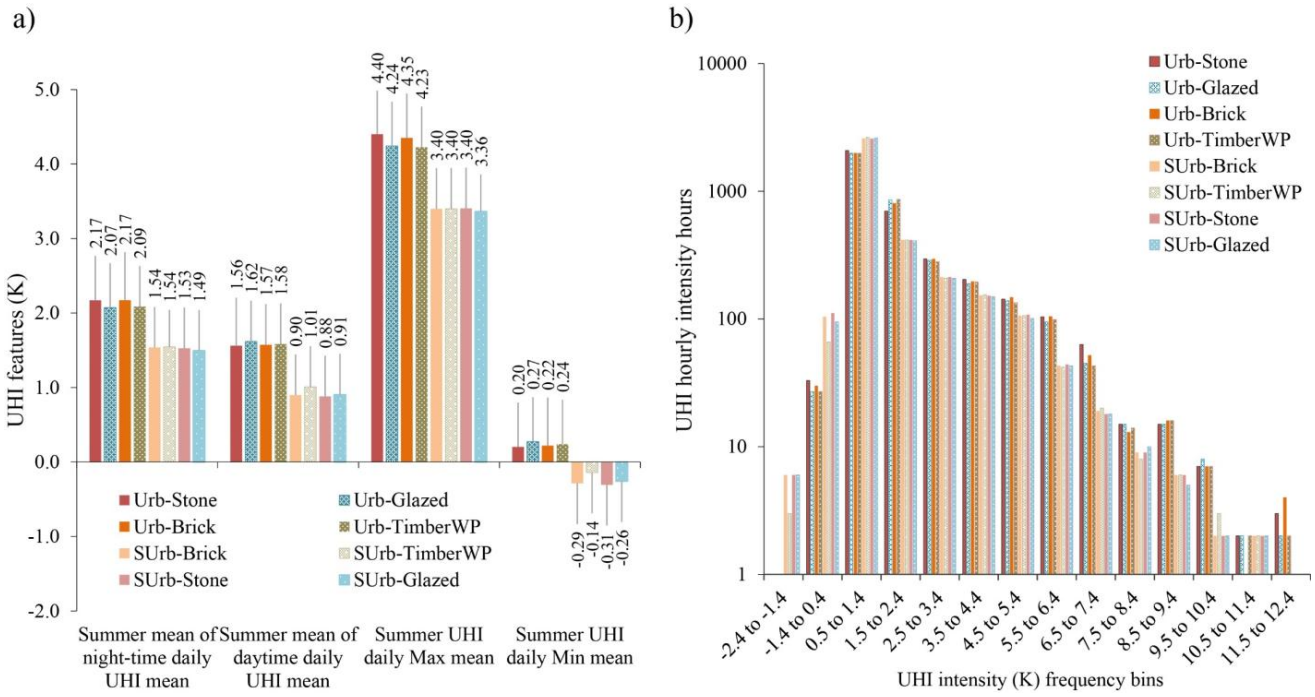

Fig. 4. Summertime (May-to-September) UHI mean features (**a**); and summertime urban and suburban UHI intensity Log_{10} frequencies (**b**) for scenarios simulated.

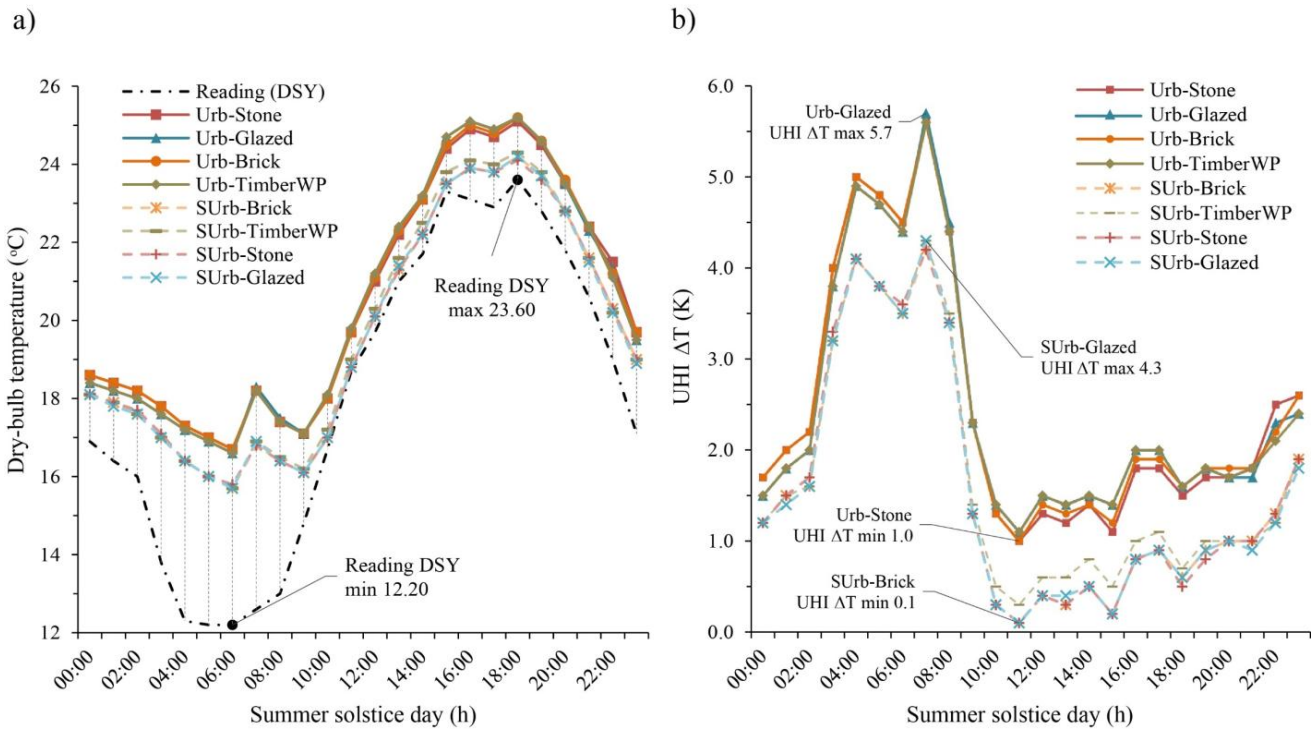

Fig. 5. Summer solstice (21-June) dry-bulb temperature profiles relative to the base Reading (DSY) profile (**a**); and summer solstice UHI ΔT (intensity) profiles (**b**) for scenarios simulated.

3.1. Canyon microclimate profiles

The summer UHI mean daily maxima for urban and suburban scenarios ranged between 3.36 and 4.40 K (SD=2.04 and 2.06, N=153), while mean daily minima ranged between -0.29 and 0.27 K (SD=0.49 to 0.52) (see Fig. 4a). Notably the latter mean daily minima for the urban scenarios presented positive values, while the suburban scenarios presented negative values to suggest greater cool island occurrences. Such cool island occurrences are indicative of this area having warmed less rapidly than the surrounding context during the period highlighted, and does not necessarily mean that an actual sink or cooling effect had occurred. When hourly resolution UHI intensity was examined, such cool island occurrences were identified in all scenarios with intensities ranging between <0 and -2.5 K representing between ~1.7 and 2.6 % for urban scenarios, while suburban scenarios showed a significantly higher proportion between 5 and 8 % of the hours simulated (N=3672). This hourly UHI ΔT resolution also identified peak values ranging between >6.5 and ≤12.5 K that represented between 2 and 3 % for urban scenarios, while for suburban scenarios it was a notably lower proportion of ~1% of the total hours simulated (see Fig. 4b). The urban Stone scenario showed the highest number of hours reaching these peak and minimum values (UHI ΔTmax =2.9 %, and ΔTmin =2.6 %) relative to Glazed and material switch scenarios of Brick and Timber. With the suburban scenarios the material switch to Stone showed the highest number of hours reaching peak values (ΔTmax =7.8 %), while Timber showed a marginal dominance for minimum values (ΔTmin =1.1 %). When hours of the day were divided to daytime (12 hours from 6 AM to 6 PM) and night-time (the residual) urban and suburban UHI intensity means, the daily daytime value ranged between 0.88 and 1.62 K (SD=0.69 and 0.83, N=153), and the night-time ranged between 1.49 and 2.17 K (SD=0.85 and 1.04). Across all scenarios night-time means were consistently higher than daytime values. However, when urban and suburban scenarios across all hours of the day were compared, a marked drop in mean intensity values were evident for the latter relative to the former.

While the above observations can be made for mean values, examining daily profiles present idiosyncratic features and deviations. For example (see Fig. 5a & b), the profiles for the summer solstice (21-June) highlighted the condition when the hourly UHI ΔT maximum for the day was reached in the morning at around 7 AM (more pronounced with urban than suburban), nearly two hours after sunrise (around 4:50 AM). The summer solstice profiles also illustrate conditions where the night-time temperatures were higher for the urban Stone scenario relative to the lightweight Glazed alternative, while the converse was true during the midday to evening period. For the corresponding suburban scenarios, the lightweight Timber scenario showed higher temperatures for the midday to evening period relative to

Brick, although a nocturnal difference was not evident. In general, the daily profiles clearly identify urban scenario UHI ΔT profiles to be considerably higher in magnitude (i.e. warmer) than corresponding suburban profiles (see Fig. 5b).

3.2. External building surface temperatures

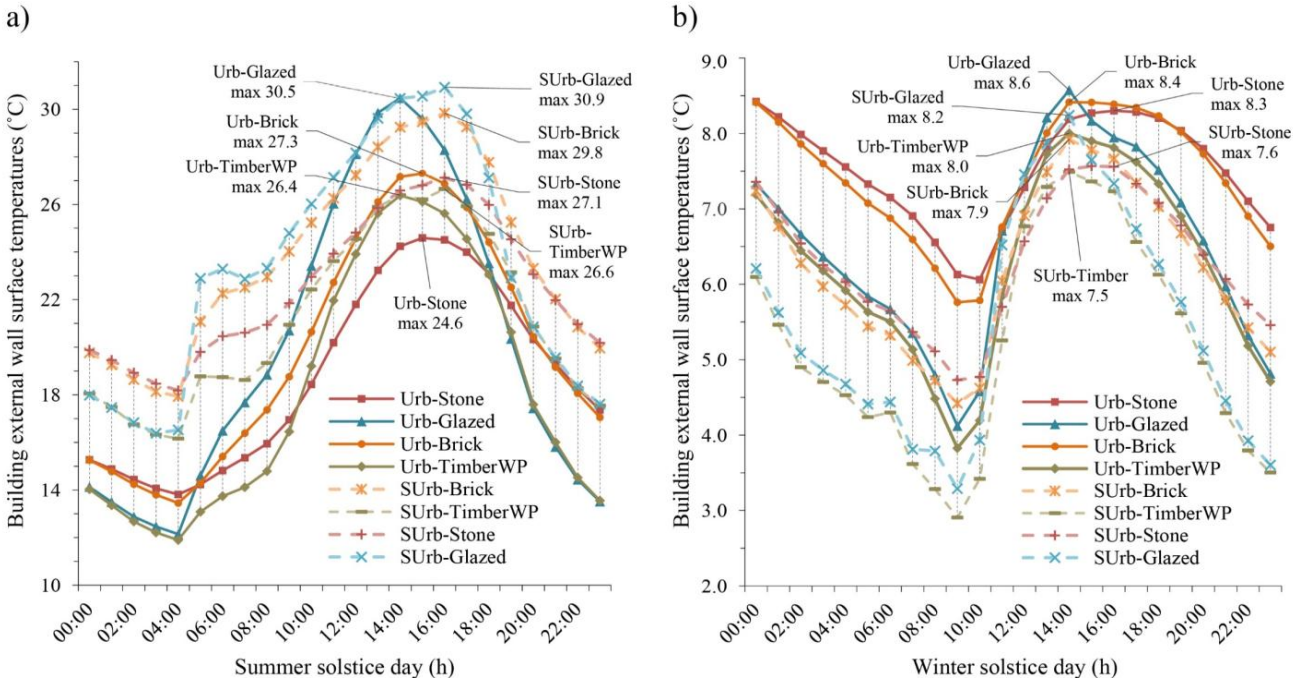

Fig. 6. Summer solstice (21-June) (**a**); and winter solstice (21-December) (**b**) building external wall surface temperatures.

When annual external surface temperature hourly means were considered for urban scenarios, Stone surfaces were marginally warmer (M=13.9 ˚C, SD=6.3, N=8760) relative to Glazed (M=13.8 ˚C, SD=7.3), while the material switch highlighted Brick to have the highest mean (M=14.2 ˚C, SD=6.7) and Timber to have the lowest (M=12.8 ˚C, SD=6.6). The profiles for both the summer and winter solstice demonstrated (see Fig. 6a & b) higher peak surface temperatures for lightweight Glazed surfaces relative to heavyweight Stone, which was notably pronounced with the summer profile. The material switch showed heavyweight Brick to generally have higher surface temperatures relative to the lightweight Timber alternative.

The corresponding annual surface temperature hourly means for the suburban scenario with Brick showed a significantly higher value (M=13.7 ˚C, SD=7.0, N=8760) relative to Timber (M=12.2 ˚C, SD=6.6), while the material switch highlighted Stone to be moderately high (M=13.2 ˚C, SD=6.4) and the Glazed switch to be marginally warmer relative to this Stone mean (M=13.4 ˚C, SD=7.5). With the summer and winter solstice profiles the peak temperature for lightweight Timber was considerably lower than the heavyweight Brick, while the material switch to lightweight Glazed had the highest peak relative to the switch to heavyweight Stone.

Notably with the summer profiles, suburban scenarios distinctly presented warmer surface temperatures during the night relative to the urban profiles, while the converse was true (though less distinct) for winter profiles. The solstice profiles also showed a temporal shift in peak temperatures for the urban Stone and material switch to Brick relative to Glazed and its corresponding switch to Timber, with one hour for the summer and two for the winter. For the corresponding suburban Brick and Timber and their material switch scenarios however, similar temporal shift was not evident (see Fig. 6a & b). A key observation to note from these surface temperature comparisons is that lightweight Glazed surfaces seem to generate higher building surface temperatures relative to other materials, particularly during periods with high solar irradiance in both urban and suburban settings.

3.3. Space-conditioning loads

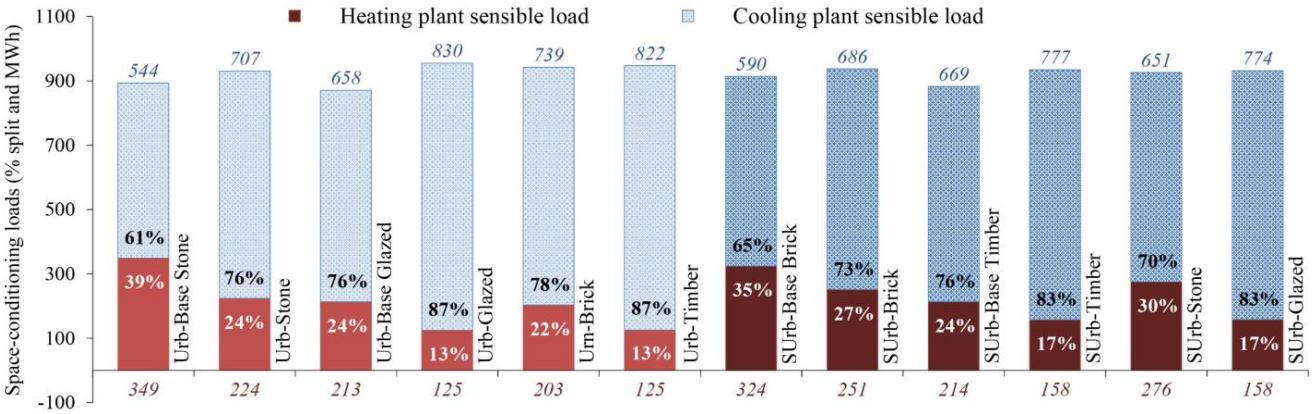

Fig. 7. Space-conditioning load comparison for scenarios simulated (all with GR: 0.30).

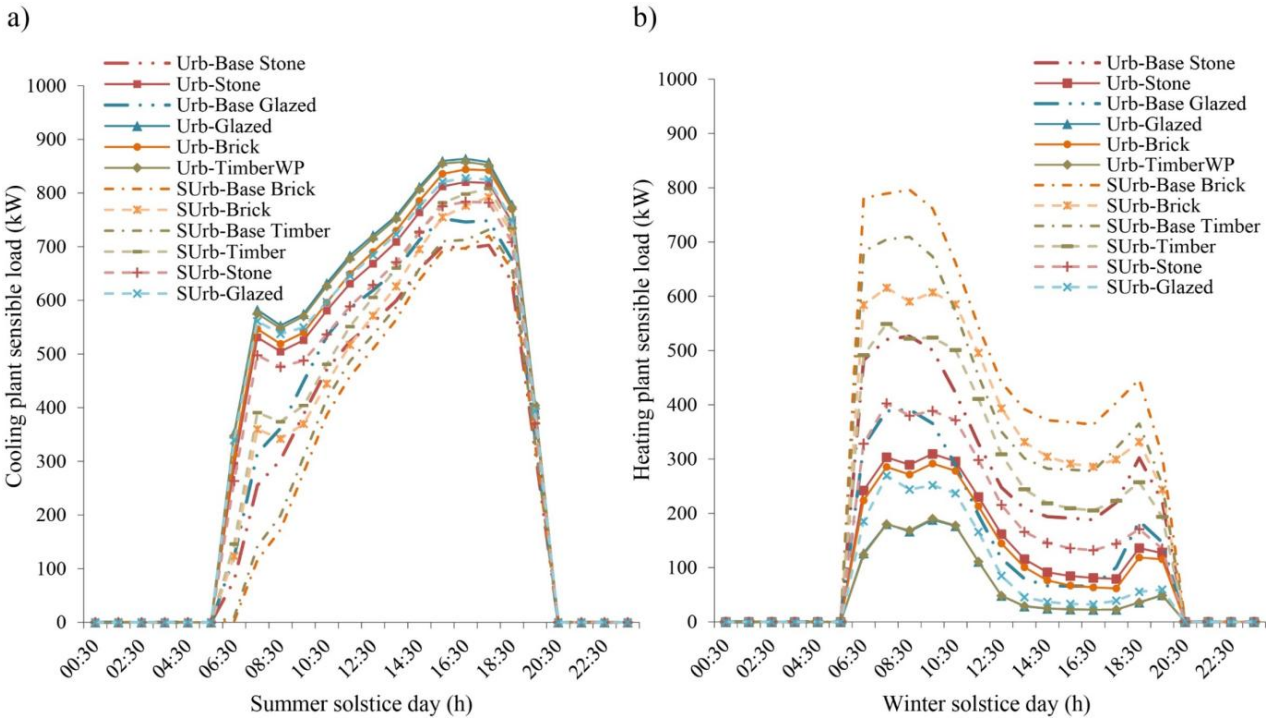

Fig. 8. Summer solstice (21-June) cooling load (**a**); and winter solstice (21-December) heating load (**b**) profiles for scenarios.

As the morphology of the suburban neighbourhood differs relative to its canyon (see Fig. 3 and Table A. 1), east and west-facing mid-canyon units were simulated to address orientation influence. The space-conditioning results showed the difference between the two orientations to be negligible with west-facing totals marginally higher (<0.2 % or <1.5 MWh) than the east-facing unit. For the remainder of the study, the suburban condition is therefore presented and discussed only in relation to west-facing unit simulations, which is consistent with the same orientation presented for the urban scenario simulations.

Including UHI influence on summer cooling and winter heating loads (see Fig. 7 & Fig. 8) demonstrated significant differences between urban and suburban scenarios. For the existing urban Stone scenario relative to its Base Stone simulation, including UHI influence resulted in a 30 % increase in summertime cooling demand, while winter heating demand was reduced by 36 %. Overall, this meant that the influence of the UHI had increased space-conditioning demand by ~38 MWh, or 4.2 %. When the urban Glazed scenario was compared against its Base Glazed simulation, UHI influence showed a 26 % increase in cooling demand and 41 % decrease in heating demand. Overall, this meant that UHI influence had increased space-conditioning demand by ~84 MWh, or 9.6 %. Hypothetical material switching

to Brick or Timber (suburban material profiles) respectively presented 1.2 and 1.8 % net increases in demand relative to existing Stone, with reductions in heating loads countered by increased cooling loads.

For the suburban Brick scenario relative to its Base Brick simulation, UHI influence resulted in a 16 % increase in summer cooling demand, while winter heating demand was reduced by 23 %. Overall, this meant that the UHI influence had increased space-conditioning demand by ~23 MWh, or 2.5 %. When the suburban Timber scenario was compared against its Base Timber simulation, UHI influence showed a 16 % increase in cooling demand and 26 % decrease in heating demand. Overall, this meant that UHI influence had increased space-conditioning demand by ~52 MWh, or 5.9 %. Hypothetical material switching to Stone or Glazed (urban material profiles) respectively presented 1.2 and 0.6 % net decreases in demand relative to existing Brick, with reductions in cooling for the Stone and heating for the Glazed contributing to net benefits.

The effect of transforming heavyweight to lightweight facades addressed by the urban comparison between Stone and Glazed scenarios (both with GR: 0.30 and UHI included), showed net annual space-conditioning demand to increase by ~24 MWh or 2.6 % for the urban office building (relative heating load reduced by 44 % and cooling load increased by 17 %). The corresponding suburban Brick to Timber comparison showed the net annual space-conditioning demand to decrease by ~3 MWh or 0.3 % for the suburban office building (relative heating load reduced by 37 % and cooling load increased by 13 %, see Fig. 7).

4. Discussion

4.1. The UHIs simulated

Considering historic observations and trends for London discussed earlier, the UHIs simulated by the UWG could be said to fall within a plausible range, with the summertime daily means for the street canyons ranging between 1.83 and 1.87 K (SD=0.86, N=153) for urban scenarios, and 1.20 and 1.27 K (SD=0.71) for suburban scenarios simulated. The suburban conditions generate a relatively milder heat island in the street canyon, which is illustrated clearly by the summer solstice profiles (see Fig. 5). This urban to suburban difference is consistent with previous observations that highlight a decrease in heat island intensity when moving away from the city centre [13], which is generally an indication of morphological spread (low density development or sprawl), and associated changes in construction types and materiality. The suggestion by Jones & Lister [18] that London's suburban areas are likely to show increasing UHIs in the future is based on the assumption of growth-related policies intensifying development density and associated material use in such areas to transform their character to a more urbanised state with increased heat storage.

When summer daytime and night-time UHI means were considered, the lower values simulated for the day relative to the night across the scenarios is consistent with previous studies that highlight the peak UHI influence as a nocturnal occurrence [2,3,17]. Howard's [2] finding of a modest relatively cooler daytime mean temperature (i.e. cool island) however was not relatable to any of the simulations. This is partly explained by the fact that cool island conditions simulated tended to be modest and restricted to shorter durations. Notably, occurrences with the urban scenarios were less than expected and limited to hourly incidences as noted in the results above. This may be attributed to the 20 m street width being wide enough to minimise the canyon shading effect (a key contributing factor), and the notably higher anthropogenic heat output used for the Moorgate area (based on Iamarino *et al.* [37] simulations) contributing to relatively higher daytime canyon temperatures. The suburban scenarios in contrast presented relatively cooler daytime temperatures, and a higher number of hours presenting cool island conditions to be experienced in the canyon. This may be attributed to the relatively lower anthropogenic heat output from the suburban context, as well as increased vegetation cover contributing to a higher proportion of the ground surface flux partitioned as latent flux (i.e. a sensible sink).

For urban scenarios, existing Stone presented the highest night-time mean UHI and the hypothetical material switch to Timber presented the lowest; while the highest daytime mean UHI was presented by the Glazed scenario and the lowest presented by existing Stone. With suburban scenarios, existing Brick and the switch to Stone tied equal for the highest night-time mean and the switch to Glazed offered the lowest; while the highest daytime mean UHI was presented by the Timber scenario and the lowest by the switch to Stone. These results suggest that fabrics with dominant heavyweight constructions such as Stone or Brick, generate a warmer heat island effect to be experienced in street canyons at night relative to corresponding lightweight variations, while the converse may be true for daytime conditions. This was further clarified when hourly profiles were reviewed, where heavyweight material profiles generated higher night-time UHI maximum occurrences, while during the daytime they also contributed to greater occurrences of cool island conditions. Such observations may be explained in relation to the thermal buffering properties offered by heavyweight and high thermal capacity materials such as stone and brick.

4.2. Facade material influence

The materiality of the urban form influences the surface energy balance by affecting both net radiation and heat storage. The radiative properties of materials are emissivity and albedo, while storage properties are affected by mass, heat capacity, and thermal conductivity. The radiative property albedo (α) is defined as the ratio of solar energy (mainly 250 to 2500 nm wavelengths) reflected by a surface, and is a significant determinant of material surface temperatures [3,5,38]. Since 43 % of solar energy is in the visible wavelengths (400 to 700 nm), material colour is strongly correlated with albedo, with lighter coloured surfaces having higher values (α >0.7) than darker surfaces (α ~0.2) [8,39]. For the urban condition, the stone was assumed to be homogenous Portland (typical for the Moorgate area), which is of a lighter colour and relatively high mean α = 0.6 [40]. With the suburban condition, the Timber was coated white to present an even higher α = 0.8 [39]. These albedos in turn contribute to lower radiation absorption by the facade material that helps to reduce their surface temperatures. As the summer (see Fig. 6a) and winter (Fig. 6b) solstice surface temperature profiles for external walls demonstrated, during the midday period the temperature is lower for urban Stone surfaces compared to Glazed (α = 0.3), and similarly the suburban Timber is lower relative to Brick (α = 0.3). Furthermore, this difference is pronounced during the summer when solar radiation influence is at its greatest. Such surface temperature differences between heavyweight and lightweight constructions can affect the urban microclimate both directly and indirectly. The direct effect is experienced in the form of its influence on reducing canyon ambient temperatures as cooler surfaces would have relatively lower sensible flux. The indirect effect works in conjunction with material emissivity and thermal storage properties to modify building energy use and eventual feedback to the external microclimate.

Higher radiation reflection from high albedo materials mean that less energy is available for transfer into their depth. From the residual energy that is absorbed, a material's ability to store heat (capacity) that at times is referred to as thermal mass, and thermal diffusivity, the ease by which heat penetrates a material (function of thermal conductivity and volumetric heat capacity), determines its thermal inertia, a measure of the responsiveness of a material to temperature variations. Heavyweight materials such as stone and brick have relatively higher diffusivity, heat capacity, and thermal inertia, which means that their temperature fluctuations through the diurnal cycle are minimised [41]. When radiation energy is received by such surfaces, the non-reflected energy is absorbed and stored, which increases the temperature of the material. As the surrounding climate cools this stored heat is re-radiated back to the local environment as longwave (thermal) infrared radiation. It is significant to note that this radiated heat is diffuse and therefore re-absorption by other surfaces within the street canyon will also contribute to the experienced temporal lag. This lag is evident when examining external surface temperature profiles (see Fig. 6), which show a lower daily variability range (amplitude) and delay in peak (phase shift) for urban Stone surfaces relative to Glazed. With the suburban profiles, the daily variability range (amplitude) is less pronounced than the urban comparison, and notably a temporal lag is not evident. This latter aspect means that the suburban scenarios seem to have greater relatability or coupling with the external microclimate relative to urban conditions, which is likely due to the reduced albedo and thickness of the brick skin relative to stone leading to higher surface temperatures and rapid radiating during the day.

Previous studies considering mostly housing have highlighted summertime overheating risk to be more frequent in buildings with lightweight constructions than those with heavyweight materials [12]. Some have stressed this risk to worsen with future climate warming scenarios and have criticised such modern lightweight solutions for offering little advantage over traditional heavyweight approaches [11,12]. The studies attribute this heightened risk to the low thermal mass presented by such lightweight constructions. The material of the envelope absorbing and storing heat (having high thermal mass) means that the direct transfer of solar thermal energy into indoor environments is both reduced and delayed. This helps to reduce daytime overheating risk and in turn any cooling loads utilised to mitigate this risk, along with concomitant heat rejection feedback to the climate. When utilised in conjunction with material heat storage in the right locations and with adequate night-time purge ventilation, heavyweight constructions could provide thermally comfortable indoor environments with reduced space-conditioning loads in both winter and summer. Optimal conditions however are dependent on not only the duration and magnitude of heating loads experienced, but also on occupancy groups and their activity schedules [11].

4.3. Building occupancy and storage lag

Occupancy groups and activity schedules are mainly discussed in literature in relation to domestic circumstances, with constructions and their materiality having significant bearing on heat related risks to building occupants. Recent studies have revealed dwelling types characterised by such parameters to play a significant role in the spatial variation of mortality risk from excess heat loads [42,43]. This risk is heightened in domestic situations during nocturnal hours [44], which may be exacerbated further in poorly ventilated dwellings with heavyweight envelopes, as well as highly insulated

and airtight lightweight envelopes. In the case of office conditions considered for the simulations of this study, nocturnal risk is minimised by predominantly daytime occupation. The lag in heat transfer offered by heavyweight constructions therefore benefit energy use objectives in the summer by reducing cooling loads when building occupation levels are at their highest, while at night the purged heat is not directly encountered by occupants. This heavyweight heat storage benefit however can have a negative effect in winter as a significant proportion of the initial energy expenditure may be used to heat the construction rather than the indoor environment. In such conditions, pre-heating (heating spaces prior to occupation) may be necessary, which in turn may affect net energy use. Lightweight constructions on the other hand demonstrate faster response to climate thermal loading, which explains their reduced winter heating loads for the scenarios simulated (see Fig. 7 and Fig. 8). Desired wintertime solar gain is therefore directly transferred to indoor environments to aid in reducing heating load demand. This is notable when examining the impact of including the UHI thermal load, which readily coupled with the indoor spaces of the building to present a significant 'winter warming effect' (41 % and 26 % reductions for urban Glazed and suburban Timber scenarios respectively). This however could present a negative impact in the summer for such lightweight constructions, where pre-cooling (cooling spaces prior to occupation) may be necessary, which in turn may affect net energy use. Be it light or heavyweight constructions, thermal storage aspects must therefore be assessed in conjunction with space-conditioning strategies and concomitant occupation schedules.

The thermal efficiencies of the building envelope have a significant bearing on the degree of benefit or detriment that the UHI load presents to their space-conditioning loads. In this study, simulated space-conditioning loads demonstrated that heavyweight Stone and Brick constructions accommodate the additional thermal load from the UHI relatively better over the course of the year than lightweight Glazed or Timber constructions with the same GR. Although such energy use benefits of using thermal storage of heavyweight structures is acknowledged by previous studies in warmer climates, net influences in temperate and cold climate conditions require further attention [45]. Some recent studies have suggested that in colder climates in particular, disadvantages may be pronounced to result in increased net energy consumption [45,46].

5. Conclusion

To assess UHI influence on building energy simulation, the methodology of this study presented the combined simulation approach of using a modified urban climate model (UWG) and a building energy model as a computationally efficient pathway. This however has a few limitations to bear in mind when considering application. The simplifications of the UWG mean that although accuracy is reasonable for neighbourhood-scale canyon temperature and humidity estimation (within 1 K), this is not sufficient to assess high-risk conditions where lower temperature variability (<1 K) could present risk to the health of vulnerable groups (e.g. overheating assessments of neighbourhoods with sheltered housing or hospitals). For such conditions a more accurate and typically computationally intensive microclimate simulation approach would need to be considered (e.g. use of CFD in the recent Toparlar *et al.* [47] study). The UWG outcome is also highly dependent on data input relevance and accuracy. If erroneous assumptions are made particularly in relation to priming rural weather data or key sensitivity parameters highlighted in Appendix: Table A. 1, this will lead to the generation of unrepresentative urban canyon weather files. Furthermore, the UWG performs no explicit calculation to account for macro-context variations in green and blue-cover and assumes the influence of the typically enhanced rural evaporative surface flux as implicit in the input rural weather data. To address this limitation, the characteristic 500 m radiuses for the case study sites were purposely selected so that they excluded and were not significantly proximate to large green-spaces and waterbodies. While it is sensible to suggest that the significant green-cover presented by Wimbledon Common and Richmond Park to influence heat island dynamics [6], that degree of specificity and complexity is beyond the scope of this simulation approach to assess. Notwithstanding these limitations, the approach presented could be applied to any location globally given the availability of representative rural climate data and building construction and operation details, as the physical principles behind the models are not tied to any single climate zone. The broad agreement of the presented study's results with previous research considering such matters is also indicative of the utility this simplified and computationally efficient approach could present to designers of the built environment, particularly for initial design estimations.

Table 2.
Influence on space-conditioning loads for scenarios simulated.

	Urban scenarios	Suburban scenarios

	Urb-Base Stone	Urb-Stone	Urb-Base Glazed	Urb-Glazed	Urn-Brick	Urb-Timber	SUrb-Base Brick	SUrb-Brick	SUrb-Base Timber	SUrb-Timber	SUrb-Stone	SUrb-Glazed
UHI influence	*	**4.2%**	†	**9.6%**	-	-	*	**2.5%**	†	**5.9%**	-	-
Heating	*	-35.9%	†	-41.4%	-	-	*	-22.5%	†	-26.3%	-	-
Cooling	*	30.0%	†	26.2%	-	-	*	16.3%	†	16.2%	-	-
Lightweight Change	-	*	-	**2.6%**	-	-	-	*	-	**-0.3%**	-	-
Heating	-	*	-	-44.2%	-	-	-	*	-	-37.3%	-	-
Cooling	-	*	-	17.4%	-	-	-	*	-	13.3%	-	-
Material Switch	-	*	-	-	**1.2%**	**1.8%**	-	*	-	-	**-1.2%**	**-0.6%**
Heating	-	*	-	-	-9.2%	-44.0%	-	*	-	-	9.6%	-37.1%
Cooling	-	*	-	-	4.5%	16.3%	-	*	-	-	-5.1%	12.8%

*|† Base scenario compared against.

Note: assumed heating fuel gas and cooling fuel electricity; negative values signify relative savings.

In the exemplar simulation study presented, the UHI load increased space-conditioning loads in all simulated scenarios to demonstrate the necessity for accounting for this load when estimating energy use in urban and suburban office buildings. The results highlighted this influence to be greatest for lightweight facade material profiles in both contexts, with the greater coupling of the external climate and indoor environments and its relation to typical office occupancy profiles contributing to this outcome. This observation generally concurs with previous research that had identified higher overheating risk in residential buildings with lightweight constructions. The trend to replace traditional heavyweight building fabrics with lightweight insulated alternatives in the context of an urban centre such as Moorgate, resulted in an estimated 2.6 % increase in net space-conditioning loads, which would in turn contribute to the UHI and thereby encourage a positive feedback loop of urban warming that could exacerbate the impacts of climate change. Within the suburban context of Wimbledon, this change estimated a modest 0.3 % decrease in space-conditioning loads to provide a marginal benefit (the temperature error margin of the UWG however means that this benefit is not significant). This suggests that in terms of office building energy use, the trend is likely to lead to significantly increased energy use profiles in dense urban centres, while in suburban locations it may lead to little-to-no benefit. For the latter suburban condition, a trend reversal material switch to heavyweight stone with greater heat storage than the existing brick estimated the highest space-conditioning reduction (1.2 %). This suggests that the current practice of using timber-framed construction in such suburban neighbourhoods as requiring further review to balance their construction speed and quality control benefits offered against long-term energy use implications.

Although specific material manifestations in terms of stone etc. were discussed in this study, the identified material properties of emissivity, albedo, heat capacity, and thermal conductivity are the determinants of how solar energy is reflected, emitted, and absorbed by urban surfaces. Alternative materials with complimenting properties could therefore present comparable outcomes (e.g. concrete shares many of the properties of stone-based construction materials). The properties of the dominant material presence in a city affects the intensity and timing of when the UHI peak is likely to be observed, and how the UHI load itself is transferred into indoor environments to affect space-conditioning performance. Future tasks of regenerating urban and suburban areas should therefore consider material choices by assessing how they affect the urban energy balance. It is also worth emphasising that surface materiality is an aspect of existing built environments that can be reasonably modified with much greater practicability than its morphology, and thus offer greater potential for heat risk mitigation and reduced building energy use.

Appendix

Table A. 1

Parameters used for simulations.

	Parameter	Moorgate (central urban)	Wimbledon (suburban)
Block	Canyon block dimensions:	L 60 × D 35 × H 24.5 m	L 60 × D 35 × H 24.5 m
	Context block dimensions:	L 60 × D 35 × H 24.5 m	L 60 × D 35 × H 10.5 m
	Mean floor height:	3.5 m	
	Assumed building use:	Medium office	
	Total office area in radius:	3,410,400 m^2	2,360,400 m^2
Simplified Base (*existing heavyweight*) constructions	Wall material and thickness:	***STONE:*** Portland stone|plaster Thickness: 0.3|0.025 m U-value: 2.33 W m^{-2} K^{-1} Surface albedo: 0.62 Emissivity: 0.90	***BRICK:*** Brick|gypsum plaster Thickness: 0.215|0.035 m U-value: 1.96 W m^{-2} K^{-1} Albedo: 0.30 Emissivity: 0.90
	Roof material and thickness:	Type: Flat roof Gravel|expanded polystyrene|concrete|ceiling tiles Thickness: 0.075|0.1|0.3|0.05 m U-value: 0.24 W m^{-2} K^{-1}	Type: Inclined roof (45°) Clay tiled|timber insulation|gypsum plasterboard Thickness: 0.015|0.1|0.25|0.015 m U-value: 0.23 W m^{-2} K^{-1}
	Glazing:	GR: 0.3 (30 %) U-value: 1.93 W m^{-2} K^{-1}	
	Initial temperature of construction:	20 °C	
	Gains: lighting and equipment:	12 and 25 W m^{-2}	
	Gains: Occupancy:	6 m^2 person^{-1}	
	Gains profile used:	@ medium office schedule †	
	Infiltration:	0.5 ach	
	Ventilation:	0.002 m^3 s^{-1} m^{-2}	
	Cooling system:	Air	
	Heating efficiency:	0.80	
	Daytime and night-time set points:	@ medium office schedule †	
	Heat rejected to canyon:	50%	25%
Roads	Material and Thickness:	Asphalt | 0.5 m	
Urban & Rural	Vegetation coverage ratio:	Urban: 0.005 Rural: 0.8	0.2 0.8
Urban area	***Mean building height****	***24.5 m***	***10.8 m***
	Horizontal building density ratio*	***0.598***	***0.480***
	Vertical to horizontal area ratio*	***0.99***	***0.35***
	Tree coverage ratio	0.001	0.080
	Non-building sensible heat rejection	22.68 W m^{-2}	1.77 W m^{-2}
	Non-building latent heat rejection	2.268 W m^{-2}	0.18 W m^{-2}
	Characteristic neighbourhood length	500 m	
	Tree and grass latent fractions	0.7 and 0.5	
	Vegetation albedo	0.25	
	Vegetation contribution start-end	April to October	
	Daytime boundary layer height	1000 m	850 m
	Night-time boundary layer height	80 m	50 m
Reference site	Latitude, longitude (for *Reading*)	51.446, - 0.957	
	Distance from study sites	~60 km due west	~52 km due west

* Key neighbourhood morphological sensitivity parameters.

† Medium office schedule: Weekdays from 7 AM to 7 PM (at 0.9 load); Saturday from 7 AM to 5 PM (at 0.4 load); and Sunday full-day (at 0.1 load).

Table A. 2
Construction parameters for lightweight material simulations.

	Parameter	Moorgate (central urban)	Wimbledon (suburban)
Simplified (*hypothetical lightweight*) constructions	Wall material and thickness	***GLAZED:*** Anti-sun glass cladding|expanded polystyrene|gypsum plasterboard Thickness: 0.010|0.1|0.025 m U-value: 0.31 W m^{-2} K^{-1} Surface albedo: 0.30 Emissivity: 0.90	***TIMBER:*** White painted sheathing|expanded polystyrene| timber frame|gypsum plasterboard Thickness: 0.02|0.1|0.025|0.025 m U-value: 0.28 W m^{-2} K^{-1} Albedo: 0.80 Emissivity: 0.90

Acknowledgment

Funding: this work was supported by a University of Bath Research Studentship.

References

[1] A. Revi, D.E. Satterthwaite, F. Aragón-Durand, J. Corfee-Morlot, R.B.R. Kiunsi, M. Pelling, D.C. Roberts, W. Solecki, Urban areas, in: Clim. Chang. 2014 Impacts, Adapt. Vulnerability. Part A Glob. Sect. Asp. Contrib. Work. Gr. II to Fifth Assess. Rep. Intergov. Panel Clim. Chang., Cambridge University Press, Cambridge, 2014: pp. 535–612.

[2] L. Howard, The climate of London : deduced from meteorological observations made in the metropolis and at various places around it, Harvey and Darton, J. and A. Arch, Longman, Hatchard, S. Highley [and] R. Hunter, London, 1833.

[3] T.R. Oke, Boundary Layer Climates, 2nd ed., Methuen, London, 1987.

[4] T.R. Oke, The Energetic Basis of the Urban Heat-Island, Q. J. R. Meteorol. Soc. 108 (1982) 1–24. doi:DOI 10.1002/qj.49710845502.

[5] H. Taha, Urban climates and heat islands: albedo, evapotranspiration, and anthropogenic heat, Energy Build. 25 (1997) 99–103. doi:10.1016/S0378-7788(96)00999-1.

[6] K.R. Gunawardena, M.J. Wells, T. Kershaw, Utilising green and bluespace to mitigate urban heat island intensity, Sci. Total Environ. 584–585 (2017) 1040–1055. doi:10.1016/j.scitotenv.2017.01.158.

[7] C.S.B. Grimmond, M. Blackett, M.J. Best, J. Barlow, J.J. Baik, S.E. Belcher, S.I. Bohnenstengel, I. Calmet, F. Chen, A. Dandou, K. Fortuniak, M.L. Gouvea, R. Hamdi, M. Hendry, T. Kawai, Y. Kawamoto, H. Kondo, E.S. Krayenhoff, S.H. Lee, T. Loridan, A. Martilli, V. Masson, S. Miao, K. Oleson, G. Pigeon, A. Porson, Y.H. Ryu, F. Salamanca, L. Shashua-Bar, G.J. Steeneveld, M. Tombrou, J. Voogt, D. Young, N. Zhang, The International Urban Energy Balance Models Comparison Project: First Results from Phase 1, J. Appl. Meteorol. Climatol. 49 (2010) 1268–1292. doi:10.1175/2010JAMC2354.1.

[8] H. Taha, H. Akbari, A. Rosenfeld, J. Huang, Residential Cooling Loads and the Urban Heat-Island - the Effects of Albedo, Build. Environ. 23 (1988) 271–283. doi:Doi 10.1016/0360-1323(88)90033-9.

[9] K. Steemers, Energy and the city: density, buildings and transport, Energy Build. 35 (2003) 3–14. doi:Pii S0378-7788(02)00075-0Doi 10.1016/S0378-7788(02)00075-0.

[10] M. Santamouris, On the energy impact of urban heat island and global warming on buildings, Energy Build. 82 (2014) 100–113. doi:10.1016/j.enbuild.2014.07.022.

[11] C. Kendrick, R. Ogden, X. Wang, B. Baiche, Thermal mass in new build UK housing: A comparison of structural systems in a future weather scenario, Energy Build. 48 (2012) 40–49. doi:10.1016/j.enbuild.2012.01.009.

[12] T.O. Adekunle, M. Nikolopoulou, Thermal comfort, summertime temperatures and overheating in prefabricated timber housing, Build. Environ. 103 (2016) 21–35. doi:10.1016/j.buildenv.2016.04.001.

[13] R. Watkins, J. Palmer, P. Littlefair, M. Kolokotroni, The London Heat Island: results from summertime monitoring, Build. Serv. Eng. Res. Technol. 23 (2002) 97–106.

[14] B.J. Moffitt, The effects of urbanization on mean temperatures at Kew observarotory, Weather. 27 (1972) 121–129.

[15] T.J. Chandler, The Climate of London, Hutchinson & Co Ltd, London, 1965.

[16] D.O. Lee, Urban warming? - An analysis of recent trends in London's urban heat island., Weather. 47 (1992) 50–56.

[17] R.L. Wilby, Past and projected trends in London ' s urban heat island, Weather. 58 (2003) 251–260. doi:10.1256/wea.183.02.

[18] P.D. Jones, D.H. Lister, The urban heat island in central London and urban-related warming trends in central London since 1900, Weather. 64 (2009) 323–327. doi:10.1002/wea.432.

[19] M. Kolokotroni, Y. Zhang, R. Giridharan, Heating and cooling degree day prediction within the London urban heat island area, Build. Serv. Eng. Res. Technol. 30 (2009) 183–202.

[20] M. Kolokotroni, R. Giridharan, Urban heat island intensity in London: An investigation of the impact of physical characteristics on

changes in outdoor air temperature during summer, Sol. Energy. 82 (2008) 986–998. doi:10.1016/j.solener.2008.05.004.

[21] K.J. Doick, A. Peace, T.R. Hutchings, The role of one large greenspace in mitigating London's nocturnal urban heat island, Sci Total Env. 493 (2014) 662–671. doi:10.1016/j.scitotenv.2014.06.048.

[22] R. Giridharan, M. Kolokotroni, Urban heat island characteristics in London during winter, Sol. Energy. 83 (2009) 1668–1682. doi:10.1016/j.solener.2009.06.007.

[23] G. Pigeon, A. Lemonsu, N. Long, J. Barrié, V. Masson, P. Durand, Urban thermodynamic island in a coastal city analysed from an optimized surface network, Boundary-Layer Meteorol. 120 (2006) 315–351.

[24] M. Kolokotroni, Y.P. Zhang, R. Watkins, The London Heat Island and building cooling design, Sol. Energy. 81 (2007) 102–110. doi:10.1016/j.solener.2006.06.005.

[25] J. Hidalgo, G. Pigeon, V. Masson, Urban-breeze circulation during the CAPITOUL experiment: observational data analysis approach, Meteorol. Atmos. Phys. 102 (2008) 223–241.

[26] S. Oxizidis, A. V Dudek, A.M. Papadopoulos, A computational method to assess the impact of urban climate on buildings using modeled climatic data, Energy Build. 40 (2008) 215–223.

[27] B. Bueno, J. Sullivan, M. Street, L. Zhang, B.T. Lopez-Pineda, J. Yang, K. Gunawardena, Urban Weather Generator (V5.1.0 beta), (2017).

[28] B. Bueno, J. Sullivan, M. Street, L. Zhang, B.T. Lopez-Pineda, Urban Weather Generator (V4.1.0), (2015).

[29] B. Bueno, L. Norford, J. Hidalgo, G. Pigeon, The urban weather generator, J. Build. Perform. Simul. 6 (2013) 269–281. doi:10.1080/19401493.2012.718797.

[30] V. Masson, A physically-based scheme for the urban energy budget in atmospheric models, Boundary-Layer Meteorol. 94 (2000) 357–397.

[31] B. Bueno, L. Norford, G. Pigeon, R. Britter, A resistance-capacitance network model for the analysis of the interactions between the energy performance of buildings and the urban climate, Build. Environ. 54 (2012) 116–125. doi:10.1016/j.buildenv.2012.01.023.

[32] B. Bueno, M. Roth, L. Norford, R. Li, Computationally efficient prediction of canopy level urban air temperature at the neighbourhood scale, Urban Clim. 9 (2014) 35–53.

[33] A. Nakano, B. Bueno, L. Norford, C.F. Reinhart, Urban Weather Generator - A novel workflow for integrating urban heat island effect within urban design process, Build. Simul. 2015. (2015).

[34] M. Eames, T. Kershaw, D. Coley, On the creation of future probabilistic design weather years from UKCP09, Build. Serv. Eng. Res. Technol. 32 (2011) 127–142. doi:10.1177/0143624410379934.

[35] T. Kershaw, M. Sanderson, D. Coley, M. Eames, Estimation of the urban heat island for UK climate change projections, Build. Serv. Eng. Res. Technol. 31 (2010) 251–263. doi:10.1177/0143624410365033.

[36] IES-VE, IES-Virtual Environment (V2017.2.0.0), (2017).

[37] M. Iamarino, S. Beevers, C.S.B. Grimmond, High-resolution (space, time) anthropogenic heat emissions: London 1970-2025, Int. J. Climatol. 32 (2012) 1754–1767. doi:10.1002/joc.2390.

[38] M.Z. Jacobson, Fundamentals of atmospheric modeling, Cambridge University Press, Cambridge, 2005.

[39] M. Santamouris, D. Kolokotsa, eds., Urban climate mitigation techniques, Routledge, 2016.

[40] T. Yates, BRE, Jordans basebed technical data sheet, Building Research Establishment (BRE) on behalf of Albion Stone, Surrey, 2017.

[41] L. Gartland, Heat islands: understanding and mitigating heat in urban areas, Routledge, Oxford, 2008.

[42] J. Taylor, P. Wilkinson, M. Davies, B. Armstrong, Z. Chalabi, A. Mavrogianni, P. Symonds, E. Oikonomou, S.I. Bohnenstengel, Mapping the effects of urban heat island, housing, and age on excess heat-related mortality in London, Urban Clim. 14 (2015) 517–528. doi:10.1016/j.uclim.2015.08.001.

[43] C. Liu, T. Kershaw, D. Fosas, A.P. Ramallo Gonzalez, S. Natarajan, D.A. Coley, High resolution mapping of overheating and mortality risk, Build. Environ. 122 (2017) 1–14. doi:10.1016/j.buildenv.2017.05.028.

[44] P. Murage, S. Hajat, R.S. Kovats, Effect of night-time temperatures on cause and age-specific mortality in London, Environ. Epidemiol. (2017) 1. doi:10.1097/EE9.0000000000000005.

[45] A. Reilly, O. Kinnane, The impact of thermal mass on building energy consumption, Appl. Energy. 198 (2017) 108–121. doi:10.1016/j.apenergy.2017.04.024.

[46] V. Stevens, M. Kotol, D. Ph, B. Grunau, C. Craven, The Effect of Thermal Mass on Annual Heat Load and Thermal Comfort in Cold Climate Construction, J. Cold Reg. Eng. 30 (2016) 1–13. doi:10.1061/(ASCE)CR.1943-5495.0000092.

[47] Y. Toparlar, B. Blocken, B. Maiheu, G.J.F. van Heijst, Impact of urban microclimate on summertime building cooling demand: A parametric analysis for Antwerp, Belgium, Appl. Energy. 228 (2018) 852–872. doi:10.1016/j.apenergy.2018.06.110.

Table 1.
Simulation scenarios considered.

	Weather file used	Constructions used
Urban (*Urb*)		
Urb-Base Stone	Unmodified Reading DSY.	*Default heavyweight scenario:* Using stone facades with glazing ratio (GR) of 0.30, detailed in Appendix: Table A. 1 (currently dominant among buildings of Moorgate).
Urb-Stone	Above modified using the UWG, i.e. with dominant construction of Stone facades and resulting UHI influence included.	
Urb-Base Glazed	Unmodified Reading DSY.	*Lightweight upgrade scenario:* Using glazed facades with GR of 0.30, detailed in Appendix: Table A. 2 (hypothetical).
Urb-Glazed	Above modified using the UWG, i.e. with dominant construction of Glazed facades and resulting UHI influence included.	
Urb-Brick	DSY for Reading modified using the UWG, i.e. with dominant construction of brick/timber facades and resulting UHI influence included.	*Material switch scenarios:* Using brick/timber facades with GR of 0.30, detailed in Appendix: Table A. 1 & Table A. 2 (hypothetical).
Urb-Timber		
Suburban (*SUrb*)		
SUrb-Base brick	Unmodified Reading DSY.	*Default heavyweight scenario:* Using brick facades with GR of 0.30, detailed in Appendix: Table A. 1 (currently dominant among buildings of Wimbledon).
SUrb-Brick	Above modified using the UWG, i.e. with dominant construction of brick facades and resulting UHI effect included.	
SUrb-Base Timber	Unmodified Reading DSY.	*Lightweight upgrade scenario:* White-painted timber facades with GR of 0.30, detailed in Appendix: Table A. 2 (hypothetical).
SUrb-Timber	Above modified using the UWG, i.e. with dominant construction of white-painted timber facades and resulting UHI effect included.	
SUrb-Stone	DSY for Reading modified using the UWG, i.e. with dominant construction of stone/glass facades and resulting UHI influence included.	*Material switch scenarios:* Using stone/glass facades with GR of 0.30, detailed in Appendix: Table A. 1 & Table A. 2 (hypothetical).
SUrb-Glass		

Note to editor: no requirement for colour in print

Table 2.
Influence on space-conditioning loads for scenarios simulated.

	Urban scenarios						Suburban scenarios					
	Urb-Base Stone	Urb-Stone	Urb-Base Glazed	Urb-Glazed	Urn-Brick	Urb-Timber	SUrb-Base Brick	SUrb-Brick	SUrb-Base Timber	SUrb-Timber	SUrb-Stone	SUrb-Glazed
UHI influence	*	**4.2%**	†	**9.6%**	-	-	*	**2.5%**	†	**5.9%**	-	-
Heating	*	-35.9%	†	-41.4%	-	-	*	-22.5%	†	-26.3%	-	-
Cooling	*	30.0%	†	26.2%	-	-	*	16.3%	†	16.2%	-	-
Lightweight Change	-	*	-	**2.6%**	-	-	-	*	-	**-0.3%**	-	-
Heating	-	*	-	-44.2%	-	-	-	*	-	-37.3%	-	-
Cooling	-	*	-	17.4%	-	-	-	*	-	13.3%	-	-
Material Switch	-	*	-	-	**1.2%**	**1.8%**	-	*	-	-	**-1.2%**	**-0.6%**
Heating	-	*	-	-	-9.2%	-44.0%	-	*	-	-	9.6%	-37.1%
Cooling	-	*	-	-	4.5%	16.3%	-	*	-	-	-5.1%	12.8%

*|† Base scenario compared against.
Note: assumed heating fuel gas and cooling fuel electricity; negative values signify relative savings.

Note to editor: no requirement for colour in print

Appendix

Table A. 1
Parameters used for simulations.

	Parameter	Moorgate (central urban)	Wimbledon (suburban)
Block	Canyon block dimensions:	L 60 × D 35 × H 24.5 m	L 60 × D 35 × H 24.5 m
	Context block dimensions:	L 60 × D 35 × H 24.5 m	L 60 × D 35 × H 10.5 m
	Mean floor height:	3.5 m	
	Assumed building use:	Medium office	
	Total office area in radius:	3,410,400 m²	2,360,400 m²
Simplified Base (*existing heavyweight*) constructions	Wall material and thickness:	***STONE:*** Portland stone|plaster Thickness: 0.3|0.025 m U-value: 2.33 W m^{-2} K^{-1} Surface albedo: 0.62 Emissivity: 0.90	***BRICK:*** Brick|gypsum plaster Thickness: 0.215|0.035 m U-value: 1.96 W m^{-2} K^{-1} Albedo: 0.30 Emissivity: 0.90
	Roof material and thickness:	Type: Flat roof Gravel|expanded polystyrene|concrete|ceiling tiles Thickness: 0.075|0.1|0.3|0.05 m U-value: 0.24 W m^{-2} K^{-1}	Type: Inclined roof (45°) Clay tiled|timber insulation|gypsum plasterboard Thickness: 0.015|0.1|0.25|0.015 m U-value: 0.23 W m^{-2} K^{-1}
	Glazing:	GR: 0.3 (30 %) U-value: 1.93 W m^{-2} K^{-1}	
	Initial temperature of construction:	20 °C	
	Gains: lighting and equipment:	12 and 25 W m^{-2}	
	Gains: Occupancy:	6 m^2 $person^{-1}$	
	Gains profile used:	@ medium office schedule †	
	Infiltration:	0.5 ach	
	Ventilation:	0.002 m^3 s^{-1} m^{-2}	
	Cooling system:	Air	
	Heating efficiency:	0.80	
	Daytime and night-time set points:	@ medium office schedule †	
	Heat rejected to canyon:	50%	25%
Roads	Material and Thickness:	Asphalt | 0.5 m	
Urban & Rural	Vegetation coverage ratio:	Urban: 0.005 Rural: 0.8	0.2 0.8
Urban area	***Mean building height****	***24.5 m***	***10.8 m***
	Horizontal building density ratio*	***0.598***	***0.480***
	Vertical to horizontal area ratio*	***0.99***	***0.35***
	Tree coverage ratio	0.001	0.080
	Non-building sensible heat rejection	22.68 W m^{-2}	1.77 W m^{-2}
	Non-building latent heat rejection	2.268 W m^{-2}	0.18 W m^{-2}
	Characteristic neighbourhood length	500 m	
	Tree and grass latent fractions	0.7 and 0.5	
	Vegetation albedo	0.25	
	Vegetation contribution start-end	April to October	
	Daytime boundary layer height	1000 m	850 m
	Night-time boundary layer height	80 m	50 m
Reference site	Latitude, longitude (for *Reading*)	51.446, - 0.957	
	Distance from study sites	~60 km due west	~52 km due west

* Key neighbourhood morphological parameters.

† Medium office schedule: Weekdays from 7 AM to 7 PM (at 0.9 load); Saturday from 7 AM to 5 PM (at 0.4 load); and Sunday full-day (at 0.1 load).

Note to editor: no requirement for colour in print

Table A. 2
Construction parameters for lightweight material simulations.

	Parameter	**Moorgate (central urban)**	**Wimbledon (suburban)**
Simplified (*hypothetical lightweight*) constructions	Wall material and thickness	***GLAZED:*** Anti-sun glass cladding|expanded polystyrene|gypsum plasterboard Thickness: 0.010|0.1|0.025 m U-value: 0.31 W m^{-2} K^{-1} Surface albedo: 0.30 Emissivity: 0.90	***TIMBER:*** White painted sheathing|expanded polystyrene| timber frame|gypsum plasterboard Thickness: 0.02|0.1|0.025|0.025 m U-value: 0.28 W m^{-2} K^{-1} Albedo: 0.80 Emissivity: 0.90

Note to editor: no requirement for colour in print